Supporting Information for

Variability in ice cover does not affect annual metabolism estimates in a small eutrophic reservoir

Dexter W. Howard[1], Jennifer A. Brentrup[2], David C. Richardson[3], Abigail S. L. Lewis[1], Freya E. Olsson[1], Cayelan C. Carey[1]

[1]Department of Biological Sciences, Virginia Tech, Blacksburg, VA, USA

[2]Minnesota Pollution Control Agency, Saint Paul, MN, USA

[3]Biology Department, SUNY New Paltz, New Paltz, NY, USA

Corresponding author: Dexter W. Howard (dwh1998@vt.edu)

Contents of this file

Texts S1 to S4
Figures S1 to S6
Tables S1 to S4

Introduction

This supplementary material includes two texts and three figures on data gap-filling discussed in the manuscript. One text, one figure, and one table provide information on alternate classification of seasons, which did not alter our results. One text and one table provide information on the changing winter simulation discussed in the discussion of the manuscript. Two figures and one table provide additional results referenced in the manuscript.

Text S1. Dissolved oxygen sensors offset

   To calculate metabolism over a near-continuous period from 9 November 2015 to 28 February 2022, we harmonized data from the InsiteIG and YSI EXO2 DO sondes. Since they were deployed at slightly different depths, 1.0 and 1.6 m respectively, and underwent different cleaning routines, we corrected the InsiteIG sonde to the YSI EXO2, which had a longer time series. We compared the five-month time period when both sensors were deployed (29 August 2018 - 31 December 2018) and calculated the difference between the two sensors at each timestep (Supplementary Figure S1). The mean difference between the sensors was 1.687 mg L^{-1}. Based on this comparison, all data from the InsiteIG DO sonde were adjusted using the offset calculation below (equation 1), which resulted in a better relationship between the two sondes over the comparison period (Supplementary Figure S1).

$$equation\ 1{:}\ DO_{corrected}\ =\ DO_{raw}\ +\ 1.687$$

Text S2. Data Gap-Filling

The metabolism model (Section 2.4) used to calculate R and GPP required continuous daily input data, necessitating multiple harmonization and interpolation approaches. We used several different modeled data sources to fill gaps in the water temperature profile data because high-frequency temperature sensors were not deployed from 15 January 2018 – 4 July 2018. From 23 April – 4 July 2018, weekly water temperature profiles at the deepest site were available and linearly interpolated to a daily timestep. Weekly water temperature profiles were collected with a YSI ProODO meter (~ 1 m intervals; YSI Inc., Yellow Springs, OH) and a 4-Hertz Conductivity, Temperature, and Depth (CTD) profiler (~0.1 m resolution; SeaBird Electronics, Bellevue, WA, USA). YSI measurements of water temperature were taken on ~1 m intervals from the surface to the bottom of FCR. The CTD profiler collected water temperature measurements at a ~0.1 m resolution from the surface to the bottom of FCR. A comparison of interpolated YSI and CTD water temperature to observed water temperature (using the NexSens T-Node FR Thermistors) for an overlapping period when data were available (6 July 2018 – 16 December 2018) had an RMSE (root mean square error) of 0.5°C across depths of 0.1, 5, 8, and 9 m. These depths were chosen for the comparison because other YSI and CTD sampling depths did not match modeled output depths.

Few YSI and CTD observations were available between 15 January 2018 – 22 April 2018. Thus, from January to April 2018, we used hourly modeled water temperature output from the General Lake Model (GLM), a process-based hydrodynamic model that had been calibrated for FCR in a previous study (Carey et al., 2022). A comparison of modeled GLM water temperature to observed water temperature (using the NexSens T-Node FR Thermistors) for an overlapping period when data were

available (1 January 2019 – 31 December 2020) across all depths (0.1, 1, 2, 3, 4, 5, 6, 7, 8, and 9 m) had an RMSE of 1.3° C.

Finally, there were several gaps in meteorological data from 2016 – 2018 that ranged from 16 days to 77 days (66 days in 2016, 77 days in 2017, and 16 days in 2018). To account for these missing data, we developed linear relationships between observed meteorological data and modeled North American Land Data Assimilation System-2 (NLDAS-2; Xia et al., 2012) data during November 2015 – December 2019 (Supplementary Figures S2 and S3). We then calculated wind speed and incoming shortwave radiation data to gap-fill the periods with missing local meteorological data (Wind speed RMSE = 2.5 m s^{-1}; Shortwave radiation RMSE = 106 W m^{-2}).

References

Carey, C. C., Hanson, P. C., Thomas, R. Q., Gerling, A. B., Hounshell, A. G., Lewis, A. S. L., et al. (2022). Anoxia decreases the magnitude of the carbon, nitrogen, and phosphorus sink in freshwaters. Global Change Biology, 28(16), 4861–4881. https://doi.org/10.1111/gcb.16228

Xia, Y., Mitchell, K., Ek, M., Sheffield, J., Cosgrove, B., Wood, E., Luo, L., Alonge, C., Wei, H., Meng, J., Livneh, B., Lettenmaier, D., Koren, V., Duan, Q., Mo, K., Fan, Y., & Mocko, D. (2012). Continental-scale water and energy flux analysis and validation for the North American land data assimilation system project phase 2 (NLDAS-2): 1. Intercomparison and application of model products. Journal of Geophysical Research: Atmospheres(117), D03109. https://doi.org/10.1029/2011JD016048

Text S3. Testing seasonal classifications

Given the numerous ways to classify seasons in lakes (e.g., Gray et al., 2020; Jane et al., 2023; Pierson et al., 2011; Rabaey et al., 2021), we tested four different classifications to confirm that our results were not biased by our definition of a season. The four different definitions we tested were: 1) Operational definitions of summer and winter (as used in the main manuscript), in which summer was defined as the earliest date of stratification onset to the latest of date of stratification breakup observed in our dataset, and winter was defined as the earliest date of ice cover to latest date of ice cover in our time series; 2) Operational definition of winter and physical definition of summer, in which winter was the same as our first definition, but the start and end of summer changed each year based on the start and end of thermal stratification defined in Section 2.5.2; 3) Physical definitions of summer and winter, in which summer was defined as in definition 2, and winter was defined as the first date of ice cover to the last day of ice cover in that given year (noting that with this definition there was no winter season in 2020); and 4) Traditional definitions of seasons based on the solar equinox and solstice (Supplementary Table S1). Together, the exploration of these classifications were motivated by numerous other studies using a range of definitions to classify seasons (e.g., Ladwig et al., 2021, Pierson et al., 2011; Rabaey et al., 2021). Given FCR's unique ice cover dynamics, consisting of inverse stratification under intermittent ice cover, we were interested in understanding how variable ice cover affects metabolism, necessitating the need for within-winter comparisons of ice-covered and open-water conditions.

We tested how these four different classifications altered our results with respect to how the inclusion of winter metabolism affects annual metabolism estimates (Figure 2). We found that changing the seasonal classifications led to minimal differences between annual estimates that included or excluded winter. Importantly, regardless of

which definition was used, there was no statistically significant difference in NEP among seasons (Supplementary Figure S4).

References

Gray, E., Mackay, E. B., Elliott, J. A., Folkard, A. M., & Jones, I. D. (2020). Wide-spread inconsistency in estimation of lake mixed depth impacts interpretation of limnological processes. Water Research, 168, 115136. https://doi.org/10.1016/j.watres.2019.115136

Jane, S. F., Mincer, J. L., Lau, M. P., Lewis, A. S. L., Stetler, J. T., & Rose, K. C. (2023). Longer duration of seasonal stratification contributes to widespread increases in lake hypoxia and anoxia. Global Change Biology, 29(4), 1009–1023. https://doi.org/10.1111/gcb.16525

Ladwig, R., Hanson, P. C., Dugan, H. A., Carey, C. C., Zhang, Y., Shu, L., et al. (2021). Lake thermal structure drives interannual variability in summer anoxia dynamics in a eutrophic lake over 37 years. Hydrology and Earth System Sciences, 25(2), 1009–1032. https://doi.org/10.5194/hess-25-1009-2021

Pierson, D. C., Weyhenmeyer, G. A., Arvola, L., Benson, B., Blenckner, T., Kratz, T., et al. (2011). An automated method to monitor lake ice phenology. Limnology and Oceanography: Methods, 9(2), 74–83. https://doi.org/10.4319/lom.2010.9.0074

Rabaey, J. S., Domine, L. M., Zimmer, K. D., & Cotner, J. B. (2021). Winter Oxygen Regimes in Clear and Turbid Shallow Lakes. *Journal of Geophysical Research: Biogeosciences*, *126*, e2020JG006065. https://doi.org/10.1029/2020JG006065

Text S4. Exploring the effects of alternate durations of ice on annual metabolism

Given that there was no significant effect of the inclusion of winter metabolism on annual NEP estimates at FCR (Figure 2b), which was likely due to the very short duration of ice cover during our six-year study (0 to 35 days of ice per winter), we were interested in determining whether a longer ice cover duration at FCR would affect the role of winter in annual metabolism estimates. Consequently, we developed simulations to test how additional days of ice cover in each winter would affect annual NEP.

First, we differentiated between ice-covered and ice-free conditions during each year of our study. As some years were missing metabolism estimates in non-winter seasons (2015, 2016, 2017, 2022), estimates of NEP under ice (2018), and ice altogether (2020), we focused on metabolism dynamics in years 2019 and 2021 for this exploratory simulation analysis.

Second, during the winters of those two years, we converted the daily NEP estimates from the observed NEP measured during ice-free winter conditions to the mean NEP rates exhibited during ice-covered conditions. We incrementally increased the number of days with simulated under-ice conditions in intervals of 1, 5, 10, 20, 40, 80, and 100 days of ice cover. To limit bias by changing previously missing values to under-ice estimates, we gap-filled days with missing NEP data to be the mean NEP observed that season (operationally defined as described in the manuscript).

Third, after generating the simulations with 1, 5, 10, 20, 40, 80, and 100 more days of ice in both 2019 and 2021, we then compared how mean estimates of NEP across these two years changed across simulations. We used Kruskal-Wallis tests to test for significant differences between mean NEP across simulations to determine if there was a threshold of additional days of ice-cover that would cause a significant change in annual mean NEP estimates. Across the simulations of 1 – 100 more days of ice, we did not observe significant changes in annual NEP estimates (Kruskal-Wallis H_7

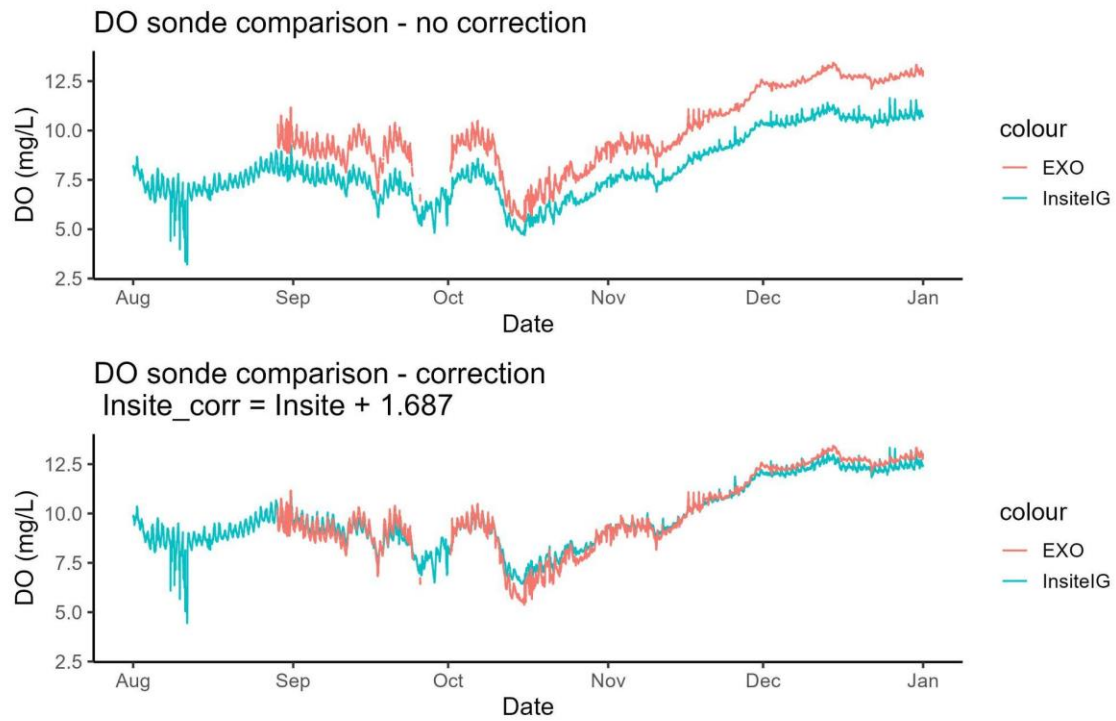= 7.91, p = 0.34; Supplementary Table S4).

Figure S1. a) Time series of DO concentration measured with the EXO2 sensor (deployed at 1.6 m) and InsiteIG sensor (deployed at 1.0 m) in 2018 before the offset was applied. b) Time series of DO from the EXO2 and InsiteIG sensors after correcting the InsiteIG data using the equation in Supplementary Text S1.
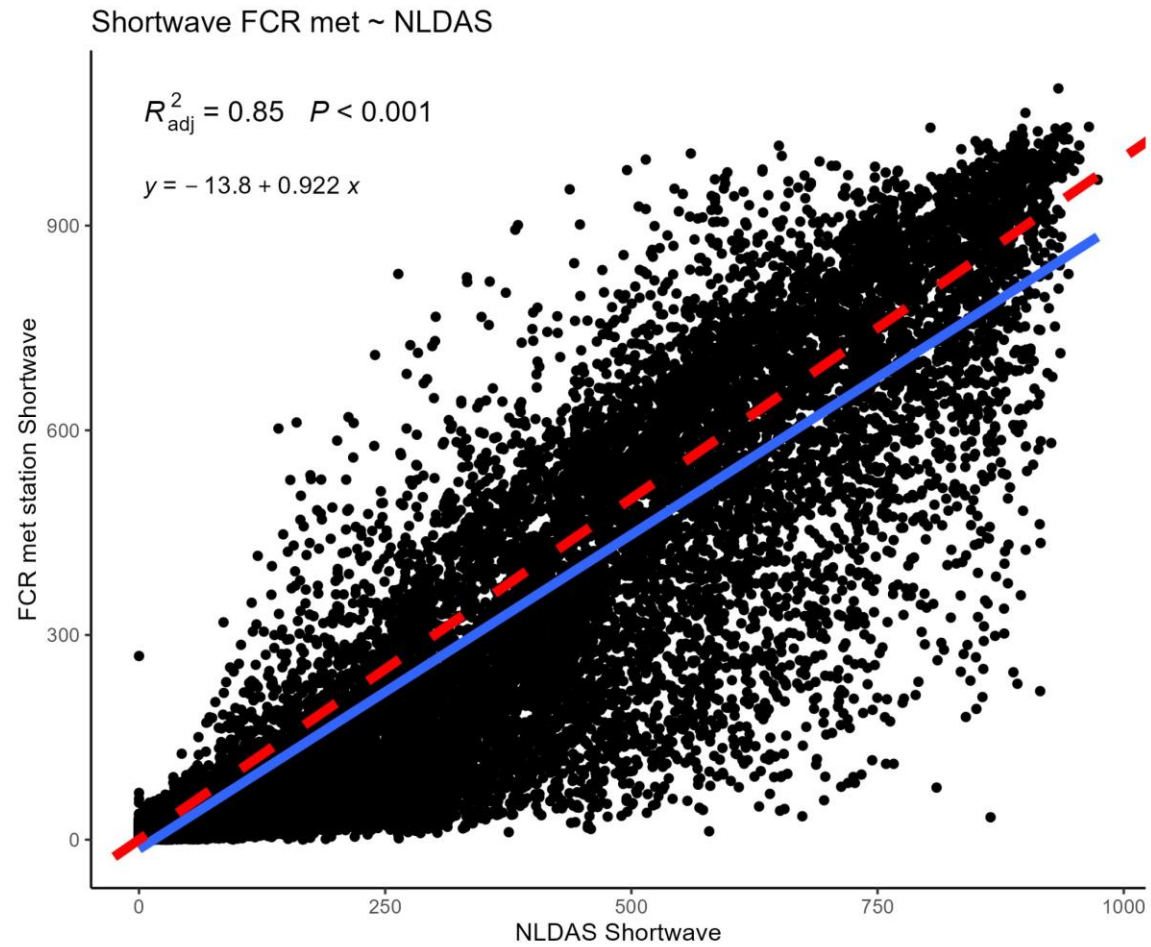
Figure S2. The solid blue line shows the correlation between observed shortwave radiation measured at the Falling Creek Reservoir meteorological station (FCR met station) and modeled shortwave radiation from the North American Land Data Assimilation System-2 (NLDAS-2). The dashed red line represents the 1:1 line of the variables.
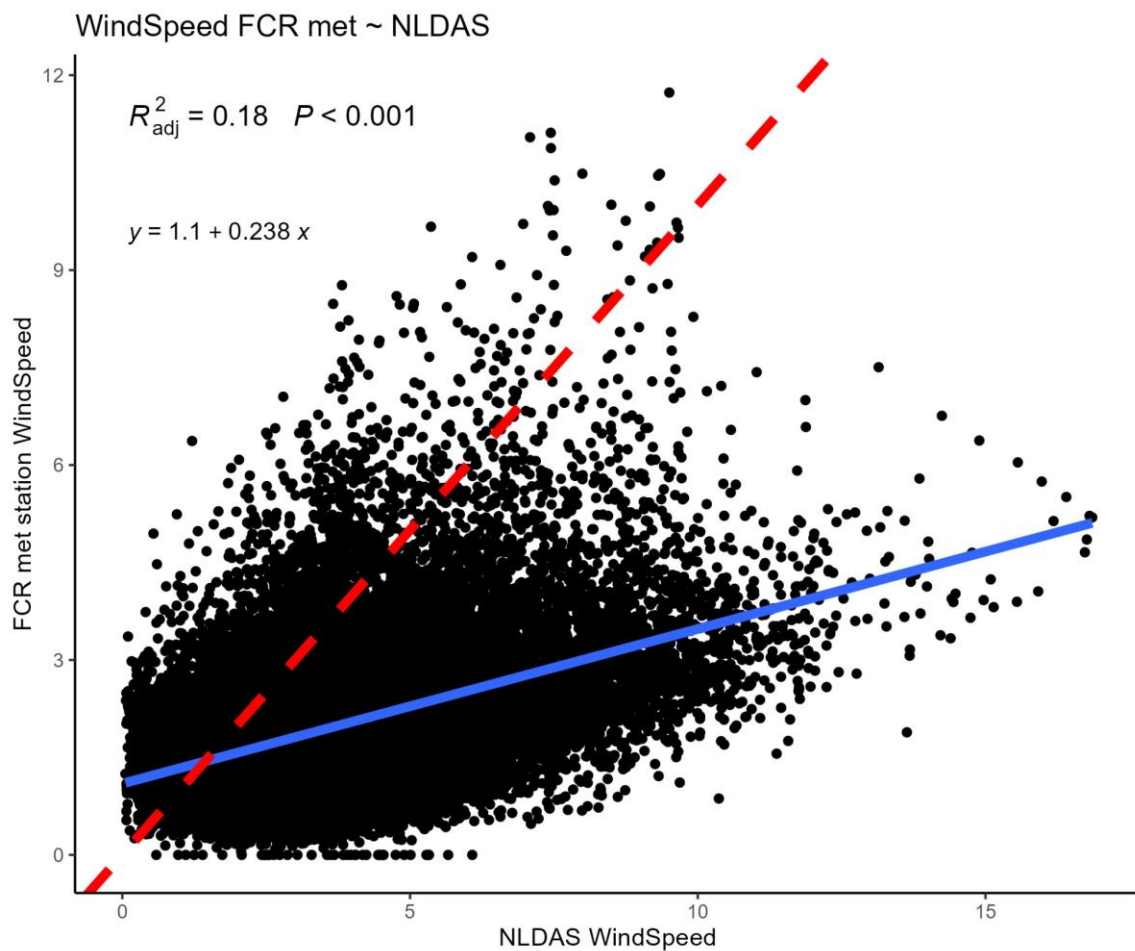
Figure S3. The solid blue line shows the correlation between the observed wind speed measured at the Falling Creek Reservoir meteorological station (FCR met station) and modeled wind speed from North American Land Data Assimilation System-2 (NLDAS-2). The dashed red line represents the 1:1 line of the variables.
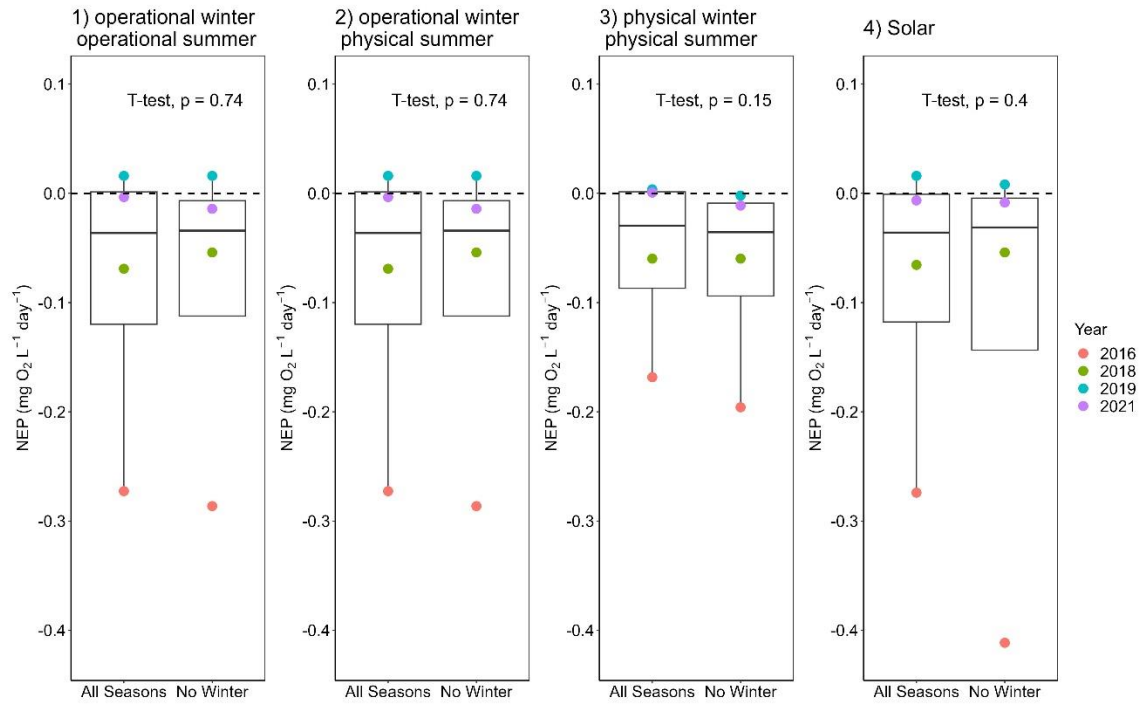
Figure S4. Boxplots comparing annual median NEP when including daily estimates from all seasons vs. when excluding winter, using different seasonal classifications described in Supplementary Text S3. Colored points denote different years. T-test text shows results from paired T-test comparing means between all seasons and no winter groupings.
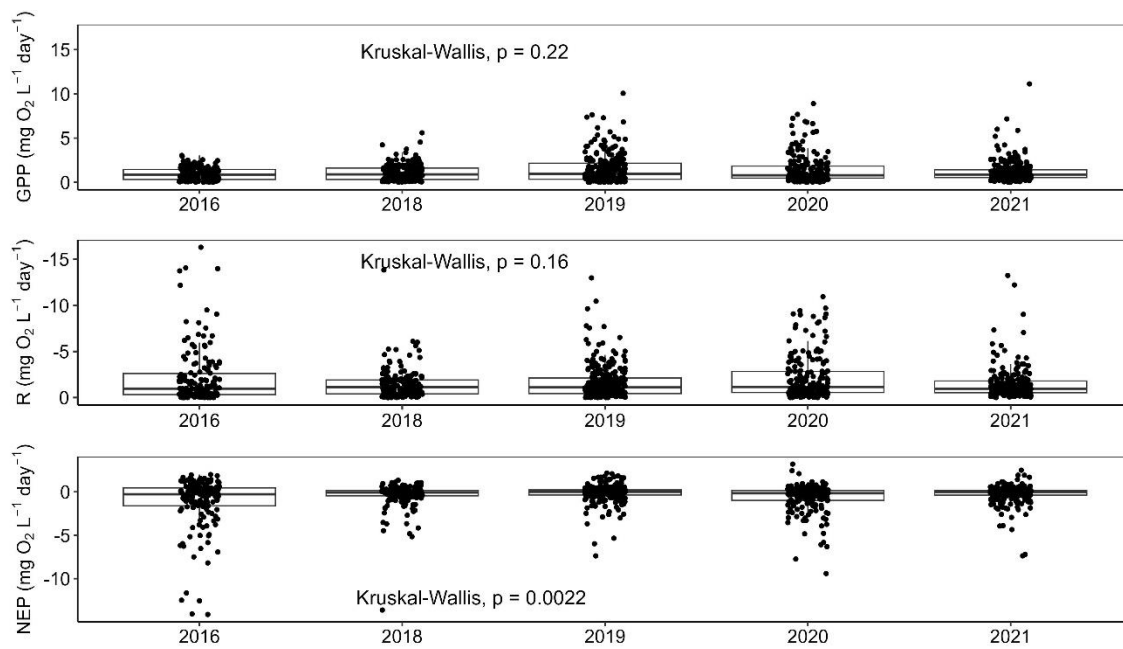
Figure S5. Boxplots comparing GPP, R, and NEP across years. 2015, 2017, and 2022 were not included since they were missing estimates for multiple seasons.
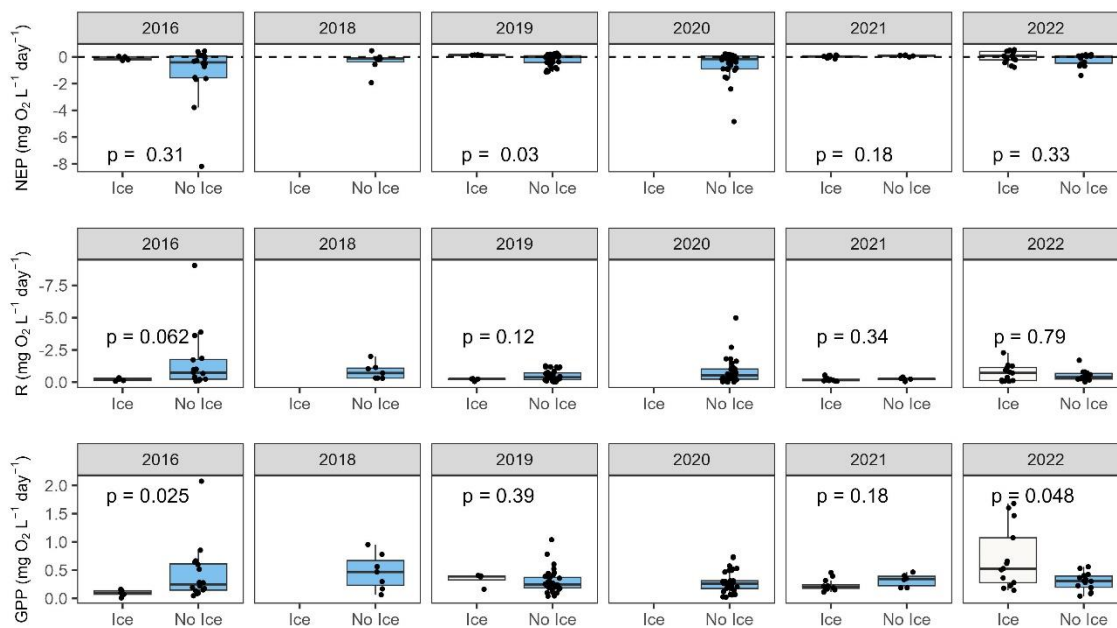
Figure S6. Boxplots of daily NEP, GPP, and R rates for each winter season comparing days with ice cover (white) and days without ice cover (blue). 2018 had no NEP estimates on days with ice cover. Winter 2020 had no ice-covered days. Wilcoxon tests were used to compare between ice covered and ice-free periods and p-values from these tests are displayed.

Table S1. Starting and ending dates for different seasons following the alternate season classifications described in Supplementary Text S1.

Classification	Year range	Start of Winter	Start of Spring	Start of Summer	Start of Fall
Operational Summer and Winter	20 December – 19 December	20 December	23 February	9 March	3 November
Operation winter and physical summer	20 December – 19 December	20 December	23 February	9 March – 25 March	14 October – 3 November
Physical summer and winter	Start of fall – end of summer	20 December – 21 January	9 January – 23 February	9 March – 25 March	14 October – 3 November
Solar	21 December – 20 December	21 December	21 March	21 June	21 September

Table S2. Median ± standard deviation (SD), range, and coefficient of variation (CV), for R, GPP, and NEP in each year with a full year of metabolism rate estimates.

Year	R			GPP			NEP		
	median ± SD (mg O_2 L^{-1} day^{-1})	range (mg O_2 L^{-1} day^{-1})	CV	median ± SD (mg O_2 L^{-1} day^{-1})	range (mg O_2 L^{-1} day^{-1})	CV	median ± SD (mg O_2 L^{-1} day^{-1})	range (mg O_2 L^{-1} day^{-1})	CV
2016	-0.97 ± 3.01	(-16.3) - 0	-1.41	0.88 ± 0.71	0 - 3.04	0.73	-0.27 ± 2.96	(-14.13) - 2	-2.57
2018	-1.14 ± 1.54	(-13.84) - 0	-1.06	0.9 ± 0.93	0.01 - 5.6	0.86	-0.07 ± 1.39	(-13.62) - 1.33	-3.81
2019	-1.1 ± 1.82	(-12.98) - 0	-1.10	0.95 ± 1.6	0 - 10.06	1.07	0.02 ± 1.06	(-7.38) - 2.16	-6.63
2020	-1.16 ± 2.37	(-10.95) - 0	-1.11	0.8 ± 1.66	0 - 8.9	1.12	-0.15 ± 1.57	(-9.41) - 3.2	-2.40
2021	-0.96 ± 1.65	(-13.24) - 0	-1.15	0.89 ± 1.22	0 - 11.13	1.01	0 ± 1.06	(-7.37) - 2.5	-4.60

Table S3. Best-fitting (within 2 AICc units of the top model), statistically-significant autoregressive models for daily GPP, R, and NEP, listed in descending order. All three models had eight candidate environmental drivers, which were z-transformed prior to analysis. GPP_{t-1}, NEP_{t-1}, and R_{t-1} are the one-day autoregressive lag terms in each metabolism model. There were no statistically-significant models for R and NEP but we retained the base autoregressive models in the table for comparison. The environmental drivers were: DOC = dissolved organic carbon, $\bar{E}_{24}$ = mean light experienced by phytoplankton, NH_4 = ammonium, NO_3 = nitrate, Precip = total daily precipitation, SRP = soluble reactive phosphorus, Temp = water temperature, TN = total nitrogen, and TP = total phosphorus.

Model	Equation	AICc	R^2	p
GPP	$GPP = 0.86 + 0.25(GPP_{t-1}) + 0.49(TN) + 0.17(\bar{E}_{24}) + 0.23(Temp)$	114.5	0.56	< 0.001
	$GPP = 1 + 0.29(GPP_{t-1}) + 0.52(TN) + 0.23(\bar{E}_{24})$	114.7	0.55	< 0.001
	$GPP = 1.02 + 0.28(GPP_{t-1}) + 0.5(TN) + 0.22(\bar{E}_{24}) + 0.1(SRP)$	114.7	0.56	< 0.001
	$GPP = 1.01 + 0.28(GPP_{t-1}) + 0.52(TN) + 0.21(\bar{E}_{24}) + 0.12(SRP) - 0.16(NH_4)$	115.8	0.57	< 0.001
	$GPP = 0.91 + 0.25(GPP_{t-1}) + 0.49(TN) + 0.18(\bar{E}_{24}) + 0.17(Temp) + 0.07(SRP)$	116.0	0.57	< 0.001
	$GPP = 0.87 + 0.24(GPP_{t-1}) + 0.51(TN) + 0.17(\bar{E}_{24}) + 0.25(Temp) - 0.08(Precip)$	116.0	0.57	< 0.001
	$GPP = 1 + 0.3(GPP_{t-1}) + 0.53(TN) + 0.22(\bar{E}_{24}) - 0.11(NH_4)$	116.4	0.55	< 0.001
	$GPP = 0.86 + 0.26(GPP_{t-1}) + 0.51(TN) + 0.17(\bar{E}_{24}) + 0.22(Temp) - 0.1(NH_4)$	116.4	0.57	< 0.001
	$GPP = 1.03 + 0.27(GPP_{t-1}) + 0.52(TN) + 0.21(\bar{E}_{24}) + 0.11(SRP) - 0.07(Precip)$	116.4	0.57	< 0.001
	$GPP = 1.02 + 0.28(GPP_{t-1}) + 0.53(TN) + 0.23(\bar{E}_{24}) - 0.06(Precip)$	116.5	0.55	< 0.001
R	$R = -0.02(R_{t-1}) - 1.5$	320.5	0.02	0.58
NEP	$NEP = -0.04(NEP_{t-1}) - 0.23$	314.9	0.02	0.55

Table S4. Changes in NEP when adding additional days of ice cover (1, 5, 10, 20, 40, 80, and 100 days) to 2019 and 2021 following methods described in Supplementary Text S4.

Year	Observed NEP	NEP +1 day	NEP +5 day	NEP +10 day	NEP +20 day	NEP +40 day	NEP +80 day	NEP +100 day
2019	-0.16	-0.16	-0.16	-0.16	-0.15	-0.13	-0.18	-0.19
2021	-0.21	-0.21	-0.21	-0.21	-0.22	-0.18	-0.12	-0.09